

# Self-assembled single-chain oligo(*p*-phenylene) amphiphiles: reversed micelles, vesicles and gels

Vladimir Sidorov,<sup>a†</sup> Trevor Douglas,<sup>b</sup> Sergey M. Dzekunov,<sup>a</sup> David Abdallah,<sup>a</sup> Bereket Ghebremariam,<sup>a</sup> Paul D. Roepe<sup>a</sup> and Stefan Matile<sup>\*a‡</sup>

<sup>a</sup> Department of Chemistry, Georgetown University, Washington, DC 20057-1227, USA.

E-mail: matiles@gusun.georgetown.edu

<sup>b</sup> Department of Chemistry, Temple University, Philadelphia, 19122-2585, USA

Received (in Cambridge, UK) 16th April 1999, Accepted 18th June 1999

The diverse supramolecular chemistry of a rigid, T-shaped single-chain amphiphile, including giant vesicles, spherical and tubular reversed micelles, and gels, is described in comparison to that of rigid-rod amphiphiles of different length.

Classical surfactants are single-chain amphiphiles that consist of a flexible lipophilic chain attached to a hydrophilic head group.<sup>1–5</sup> To better organize their dynamic micellar or vesicular suprastructures, design and synthesis of single-chain amphiphiles with either very short (< 11 Å)<sup>2,4</sup> or very long (rod-coil polymers)<sup>6</sup> rigid-rod subunits have been the subject of recent pioneering reports. Despite the potential importance for modern-day nanotechnology and biophysics, comparable studies with oligomeric rigid-rod single-chain amphiphiles are rare, presumably because of the formidable synthetic challenges involved.<sup>7–9</sup> We have recently considered self-assembly of oligo(*p*-phenylene) amphiphiles (e.g. **1–4**, Fig. 1) as a possible explanation for the poor binding of rigid-rod guests with either asymmetric (e.g. **1**) or hydrophobically mismatched (e.g. **3**, **4**) scaffolds to lipid bilayer hosts.<sup>8–11</sup> Here we report self-assembly of 'rigid-T' single-chain amphiphile **1** into giant vesicles (**1<sub>v</sub>**), reversed micelles (**1<sub>m</sub>**), and aqueous gels (**1<sub>g</sub>**) in comparison to amphiphilic oligo(*p*-phenylene) rods of different length (**2–4**) that yield vesicles only.

'Rigid-rod' vesicles **1<sub>v</sub>**–**3<sub>v</sub>** were prepared with entrapped HPTS (8-hydroxypyrene-1,3,6-trisulfonic acid, a water soluble fluorescence probe). To obtain vesicles, fully hydrated mixed micellar solutions containing **1–4** (2 mM), octyl D-glucopyranoside (70 mM), HPTS (100 μM), and buffer (5–10 mM Na<sub>n</sub>H<sub>3–n</sub>PO<sub>4</sub>, 0–100 mM NaCl, pH 6.4) were dialysed at 60–70 °C to remove detergent and external HPTS.<sup>9–11</sup> On the other hand, reversed micelles **1<sub>m</sub>** were made from a solution of 'rigid-T' amphiphile **1** in biphasic systems composed of a nonpolar solvent (e.g. CHCl<sub>3</sub>, CH<sub>2</sub>Cl<sub>2</sub>, xylene) and either acidic (pH 1, **1<sub>m(a)</sub>**) or basic (pH 13, **1<sub>m(b)</sub>**) water with HPTS. After brief sonication, rhythmical shaking (1 h, 1300 rpm), and centrifugation (10 min, < 3000g), most of the aqueous layer was a milky, foamlike emulsion. This emulsion was stable for more than two weeks but transformed into a gel (**1<sub>g</sub>**, gel point: 1.0 mg ml<sup>-1</sup>)<sup>12</sup> within 3–5 h after removal of the organic phase containing micellar **1<sub>m</sub>**.

The spectroscopic changes of rigid-rod chromophores **1–4** upon self-assembly, namely hypo-/hypsochromism of the <sup>1</sup>L transitions and bathochromic shifts for emission maxima, are listed in Table 1. The effects reached from minor changes for 'rigid T's' (**1<sub>v</sub>**/**1<sub>m</sub>**) to unambiguous H-aggregation<sup>13</sup> for rigid rods **2<sub>v</sub>** and **3<sub>v</sub>**. This implied herringbone-type packing for self-assembled rods of 30 to 40 Å length with multiple constructive π–π-interactions at least for the latter case. An increased

tendency toward herringbones for longer rods may further account for crystallization (**4<sub>c</sub>**) instead of vesiculation of decyl(*p*-phenylene) **4** under identical conditions.

Consistent with the spectroscopic trends, differential scanning calorimetry (DSC) gave phase transitions for **1<sub>v</sub>** but not for **2<sub>v</sub>**, **3<sub>v</sub>** and **4<sub>c</sub>**. No distinct transitions for **1<sub>g</sub>** indicated that vesicular **1<sub>v</sub>** and the (according to cross-polarizing optical microscopy) amorphous crystalline gel strands in **1<sub>g</sub>** were of different nature. Studies of the presumably involved bilayers with (Fig. 1a) or without (Fig. 1b) interdigitating 'T's' are ongoing to delineate the usefulness of rigid-T vesicles **1<sub>v</sub>** with

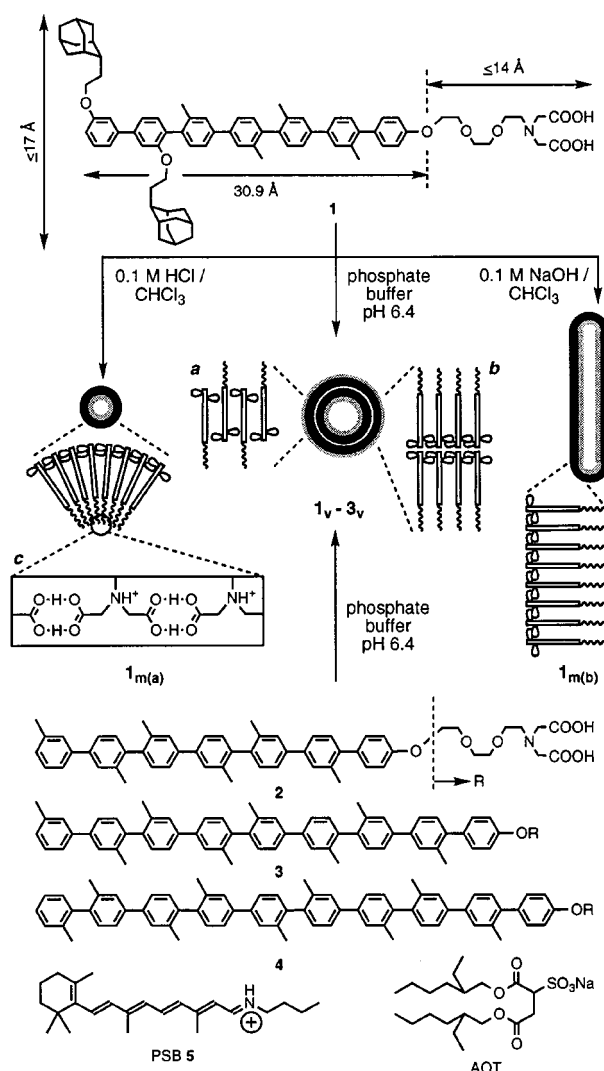


Fig. 1 Structure of oligo(*p*-phenylene)s **1–4**, PSB **5**, and AOT; schematic suprastructures for vesicular (**1<sub>v</sub>**–**3<sub>v</sub>**) and micellar (**1<sub>m</sub>**) self-assemblies.

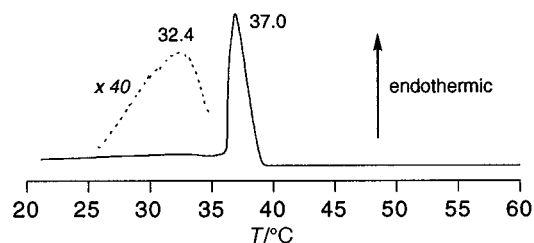
† Present address: Department of Chemistry, University of Maryland, College Park, MD, USA.

‡ Present address: Department of Organic Chemistry, University of Geneva, Geneva, Switzerland.

**Table 1** Spectroscopic data for self-assembled amphiphilic oligo(*p*-phenylene)s

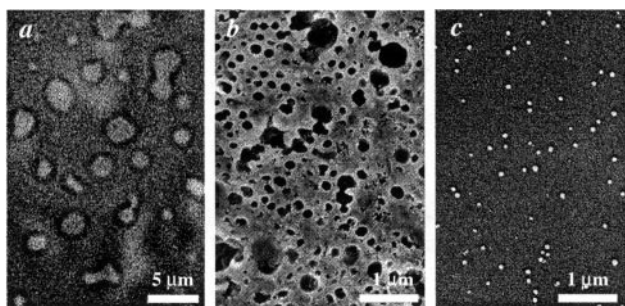
	$l^a/\text{\AA}$	Micrographs <sup>b</sup>	$\lambda^e_{\text{max}}/\text{nm}$ ( $\Delta\lambda^e_{\text{max}}/\text{nm}$ ) <sup>c</sup>	$\lambda^a_{\text{max}}/\text{nm}$ ( $\Delta\lambda^a_{\text{max}}/\text{nm}$ ) <sup>d</sup>	Hypo. <sup>e</sup>
<b>1<sub>m(a)</sub></b>	30.9	Micelles	372 (+2)	288 (−2)	0.70
<b>1<sub>v</sub></b>	30.9	Vesicles	375 (+5)	288 (−2)	0.71
<b>2<sub>v</sub></b>	30.9	Vesicles	386 (+19)	274 (−12)	0.43
<b>3<sub>v</sub></b>	39.4	Vesicles	374 (+9)	276 (−10)	0.53
<b>4<sub>c</sub></b>	43.6	Microcrystals	369 (+2)	258 (−28)	0.20

<sup>a</sup> Calculated length of rigid-rod subunit. <sup>b</sup> SEM, phase-contrast and/or fluorescence microscopy. <sup>c</sup>  $\lambda^e_{\text{max}}$ : emission maxima,  $\Delta\lambda^e_{\text{max}}$ :  $\lambda^e_{\text{max}}$  of self-assembly −  $\lambda^e_{\text{max}}$  of monomer in THF. <sup>d</sup>  $\lambda^a_{\text{max}}$ : absorption maxima,  $\Delta\lambda^a_{\text{max}}$ :  $\lambda^a_{\text{max}}$  of self-assembly −  $\lambda^a_{\text{max}}$  of monomer in THF. <sup>e</sup> Hypochromism ( $\epsilon^a_{\text{max}}$  of self-assembly/ $\epsilon^a_{\text{max}}$  of monomer in THF).

**Fig. 2** DSC heating curve of **1<sub>v</sub>** (scanning rate 1 °C min<sup>−1</sup>).

$T_c = 37.0$  °C for applications such as temperature-controlled drug release (Fig. 2).

Optical fluorescence and phase-contrast micrographs contained mainly spherical microparticles for **1<sub>v</sub>**–**3<sub>v</sub>** and **1<sub>m(a)</sub>** with average diameters that increased with scaffold length and asymmetry (**2<sub>v</sub>** < **3<sub>v</sub>** < **1<sub>m(a)</sub>** < **1<sub>v</sub>**, Fig. 3a). Microcrystals were observed for **4<sub>c</sub>**. Perhaps due to better resolution or, more likely, shrinking *in vacuo*, scanning electron microscopy (SEM) revealed nanoparticles for both ‘rigid-T’ vesicles (**1<sub>v</sub>**, Fig. 3b) and reversed micelles (**1<sub>m(a)</sub>**, Fig. 3c). Interestingly, vesicles (**1<sub>v</sub>**) appeared as cavities within precipitated  $\text{Na}_n\text{H}_{3-n}\text{PO}_4$  buffer. The additional presence of ‘8-shaped’ besides spherical vesicles implied facile fusion and fission (Fig. 3a/b).

**Fig. 3** Representative scanning electron and phase-contrast/fluorescence micrographs for self-assembled **1**–**3**. (a) Fluorescence micrograph for **3<sub>v</sub>** (diameters: 1.7–3.3 μm). (b) Scanning electron micrograph for **1<sub>v</sub>** (diameters: 80–260 nm). (c) Scanning electron micrograph for **1<sub>m(a)</sub>** (diameters: 33–73 nm).

Compatibility with the harsh SEM-conditions indicated both stability and high water permeability. The latter was supported for **1<sub>m(a)</sub>** in  $\text{CDCl}_3$  by a water exchange rate of  $k = 1.7 \text{ ms}^{-1}$  calculated from coalescence of the resonances for intracellular bulk water (4.78 ppm,  $\omega([\text{H}_2\text{O}]/[\text{I}]) \approx 100$ ) and extracellular acidic water (2.18 ppm) at 37.5 °C in the 300 MHz <sup>1</sup>H NMR spectra. Extraordinary stability of reversed micelles **1<sub>m(a)</sub>** was further implied by the constant emission intensity of encapsulated HPTS upon dilution of **1<sub>m(a)</sub>**. Apparently, the critical micelle concentrations (cmc) of **1<sub>m(a)</sub>** for formation (2 mM) and destruction (< 5 μM) differ significantly. Since rod-shaped **2**–**4** did not self-assemble under identical conditions, the T-shaped structure of **1** seems essential for micellization.<sup>3</sup> However, rapid destruction of **1<sub>m(a)</sub>** by addition of  $\text{CuCl}_2$ , as well as a wormlike morphology for ‘basic reversed micelles’ **1<sub>m(b)</sub>** (not shown) suggested additional importance of hydrogen bonding in between the hydrophilic iminodiacetate (IDA) termini of **1** for

suprastructural organization and stabilization of **1<sub>m(a)</sub>** (Fig. 1c).

Preliminary studies on reversed micelles **1<sub>m(a)</sub>** as biomimetic receptor models revealed that protonated *N*-retinylidene-*n*-butylamine Schiff base (PSB) **5** bound to **1<sub>m(a)</sub>** is not hydrolyzed by intracellular bulk water.<sup>5</sup> The absorption maximum of PSB **5** surrounded by rigid-rod arene-arrays of the supramolecular host **1<sub>m(a)</sub>** at 456 nm is 16 nm red-shifted compared to that of **5** within conventional AOT reversed micelles.<sup>14</sup> This observation reinforces the potential of **1<sub>m(a)</sub>** as valuable biomimetic receptors. It is in support of the hypothesis that fine-tuning of the absorption of retinylidene Schiff base in bacteriorhodopsins may be governed by aromatic residues in the PSB binding pocket and/or by ring-chain coplanarization of PSB in addition to external point charges.<sup>15§</sup>

In summary, our results imply that single-chain ‘rigid-T’ amphiphiles are unique surfactants with suprastructural diversity beyond the limitations of comparable rigid-rod amphiphiles. Preliminary results with remarkably stable, water permeable, reversed micelles as biomimetic receptors and catalysts implied potential usefulness of ‘rigid-T’ amphiphiles in biological, organic and materials chemistry.

This research was supported by NIH (GM56147 (SM) and GM54516 (PDR)), an award from Research Corporation (SM), the donors of the Petroleum Research Fund, administered by the American Chemical Society (SM), Suntory Institute for Bio-organic Research (SUNBOR Grant (SM)), and Georgetown University. The authors thank Drs Naomi Sakai and Richard G. Weiss for discussion, and Dr Robert E. Bachman for access to DSC.

## Notes and references

§ The effect of **1<sub>m(a)</sub>** (160 μM in  $\text{CH}_2\text{Cl}_2$ ) on the stereoselectivity of cyclopentadiene dimerization (*i.e.* an increasing relative yield of the *exo*-product from 14% to 27%) did not exceed the ordinary influence of reversed micelles.

- J.-H. Fuhrhop and J. Köning, *Membranes and Molecular Assemblies: The Cytokinetic Approach*, The Royal Society of Chemistry, Cambridge, UK, 1994.
- T. Kunitake, *Angew. Chem., Int. Ed. Engl.*, 1992, **31**, 709.
- J. Israelachvili, *Intramolecular & Surface Forces*, 2nd edn., Academic Press, London, UK, 1991.
- F. M. Menger and J. Ding, *Angew. Chem., Int. Ed. Engl.*, 1996, **35**, 2137.
- A. Singh, C. Sandorfy and J. Fendler, *J. Chem. Soc., Chem. Commun.*, 1990, 233.
- S. A. Jenekhe and X. L. Chen, *Science*, 1998, **279**, 1903.
- J. M. Tour, *Chem. Rev.*, 1996, **96**, 537.
- B. Ghebremariam, V. Sidorov and S. Matile, *Tetrahedron Lett.*, 1999, **40**, 1445.
- B. Ghebremariam and S. Matile, *Tetrahedron Lett.*, 1998, **39**, 5335.
- M. M. Tedesco, B. Ghebremariam, N. Sakai and S. Matile, *Angew. Chem., Int. Ed.*, 1999, **38**, 540.
- C. Ni and S. Matile, *Chem. Commun.*, 1998, 755.
- P. Terech and R. G. Weiss, *Chem. Rev.*, 1997, **97**, 3133.
- B. Ghebremariam and S. Matile, *Enantiomer*, 1999, **4**, 127 and 139.
- Y. Gat and M. Sheves, *J. Am. Chem. Soc.*, 1993, **115**, 3772.
- H. Houjou, Y. Inoue and M. Sakurai, *J. Am. Chem. Soc.*, 1998, **120**, 4459.

Communication 9/03041G